Follow us @BoneJointRes

Freely available online OPEN ACCESS

BJR

BIOMECHANICS

Relative movement on the articular surfaces of the tibiotalar and subtalar joints during walking

C-B. Phan, D-P. Nguyen, K. M. Lee, S. Koo

Chung-Ang University, Seoul, South Korea

Objectives

The objective of this study was to quantify the relative movement between the articular surfaces in the tibiotalar and subtalar joints during normal walking in asymptomatic individuals.

Methods

3D movement data of the ankle joint complex were acquired from 18 subjects using a biplanar fluoroscopic system and 3D-to-2D registration of bone models obtained from CT images. Surface relative velocity vectors (SRVVs) of the articular surfaces of the tibiotalar and subtalar joints were calculated. The relative movement of the articulating surfaces was quantified as the mean relative speed (RS) and synchronization index (SI_{ENT}) of the SRVVs.

Results

SI_{ENT} and mean RS data showed that the tibiotalar joint exhibited translational movement throughout the stance, with a mean SI_{ENT} of 0.54 (SD 0.21). The mean RS of the tibiotalar joint during the 0% to 20% post heel-strike phase was 36.0 mm/s (SD 14.2), which was higher than for the rest of the stance period. The subtalar joint had a mean SI_{ENT} value of 0.43 (SD 0.21) during the stance phase and exhibited a greater degree of rotational movement than the tibiotalar joint. The mean relative speeds of the subtalar joint in early (0% to 10%) and late (80% to 90%) stance were 23.9 mm/s (SD 11.3) and 25.1 mm/s (SD 9.5), respectively, which were significantly higher than the mean RS during mid-stance (10% to 80%).

Conclusion

The tibiotalar and subtalar joints exhibited significant translational and rotational movement in the initial stance, whereas only the subtalar joint exhibited significant rotational movement during the late stance. The relative movement on the articular surfaces provided deeper insight into the interactions between articular surfaces, which are unobtainable using the joint coordinate system.

Cite this article: *Bone Joint Res* 2018;7:501–507.

Keywords: Kinematics, Foot and ankle, Relative movement on surface

■ C-B. Phan, MS, Graduate Student,
■ D-P. Nguyen, MS, Researcher,
■ S. Koo, PhD, Associate Professor, School of Mechanical Engineering, Chung-Ang University, Seoul, South Korea.
■ K. M. Lee, MD, PhD, Associate Professor, Department of Orthopedic Surgery, Seoul National University Bundang Hospital, Seongnam, South Korea.

Correspondence should be sent to S. Koo;
email: skoo@cau.ac.kr

doi: 10.1302/2046-3758.78.BJR-2018-0014.R1

Bone Joint Res 2018;7:501–507.

Introduction

Joint kinematics are an important biomarker and are useful to predict the progression of degenerative joint diseases such as osteoarthritis.[1] The ankle joint complex, which bears the equivalent of approximately six times the body weight while walking,[2] consists of the tibiotalar and subtalar joints with many complex geometries. The kinematics of the tibiotalar and subtalar joints are influenced by the geometries of the articular surfaces and ligamentous structures,[3] which produce different patterns of movement during open and closed chain activities.[4] Abnormal kinematics of the ankle joint complex have been shown to contribute to the development of overuse injuries in the lower limbs.[5] Likewise, chronic ankle instability is due to a combination of mechanical and functional instability,[6] further emphasizing the importance of a thorough understanding of the corresponding joint kinematics.

The kinematics of a joint can be represented in several different ways. The kinematics of the tibiotalar and subtalar joints have been described as comprising three

Fig. 1

A biplanar fluoroscopic imaging system was set up on both sides of a walkway made of high-strength polystyrene foam to capture high-speed fluoroscopic images of the ankle joint complex from heel-strike to toe-off during normal walking.

rotational and three translational movements using an anatomical coordinate system attached to the tibia, talus, and calcaneus during simulated walking,[7,8] treadmill walking,[9] and ground walking[10-12] in 'normal' (i.e. healthy) subjects. The kinematics of the ankle joint complex are also frequently reported using a helical axis method and axis-angle representation,[13] which utilizes a 3D rotational axis and the amount of rotation around the axis of a body with respect to another body over a finite time interval. Previous studies have shown that the rotation axis of the tibiotalar is relatively consistent between subjects,[13] while that of the subtalar joint can vary substantially between subjects during gait[11] and static poses.[13,14] Thus, although both the joint coordinate system and the helical axis can be used to represent the 3D kinematics between two adjacent bones in a joint, neither system provides information about the relative movement on articulating surfaces, which is important for understanding the pathomechanics of degenerative joint disease.[1,15,16]

The biplanar fluoroscopic method for measuring 3D skeletal kinematics was recently described,[8,10,17] and allows for state-of-the-art accuracy for quantifying joint kinematics during natural movement, as well as eliminating the skin movement artefacts associated with marker-based movement capture systems.[18] Specifically, the 3D-to-2D registration method of biplanar fluoroscopic systems calculates 3D transformation matrices of individual bone models, from which either the joint coordinate system[8,10] or helical axis can be used to quantify joint kinematics.[13,14] Furthermore, by virtue of its ability to obtain highly accurate measurements, the biplanar fluoroscopic method allows for calculation of bone-to-bone distances of articulating surfaces.[9]

Surface relative velocity vectors (SRVVs) are an intuitive method for visualizing velocity fields on a contact surface and allow for improved understanding of surface-to-surface interactions that cannot be quantified using only coordinate systems embedded in the bones in traditional joint kinematics graphs. Anderst et al[19] calculated SRVVs on contacting surfaces at the level of the subchondral bone surface using the bone-to-bone distance in two consecutive frames to describe the surface contact phenomenon in a canine knee during treadmill walking. They also suggested the use of an 'inter-velocity vector angle' to quantify SRVVs in the medial and lateral compartments of the knee, although the inter-velocity vector angle changes depending on the number of samples and locations of SRVVs.

The purpose of this study was twofold. First, we attempted to quantify SRVVs using a polar histogram-based method to define velocities and rotational movement. Second, we quantified the kinematics in the tibiotalar and subtalar joints using the newly suggested SRVV quantification methods. Using these data, we evaluated differences in kinematic patterns according to different phases of normal walking in normal subjects.

Materials and Methods

Biplanar fluoroscopic data acquisition. A total of 18 healthy male subjects who provided informed consent participated in our study. The study protocol, including CT and fluoroscopic imaging, was approved by the Institutional Review Board at Chung-Ang University, Seoul, South Korea (Approval No. 14-0098, in July 2014). The mean age, height, and weight of the study subjects were 23.2 years (SD 1.8), 173.2 cm (SD 5.7), and 70.9 kg (SD 6.4), respectively. All subjects were free of pain and injury of the lower limbs for at least five years prior to enrolling in the study, and there were no cases of abnormal deformities in the ankle joint complex. All subjects underwent CT imaging. The CT data were processed using a segmentation program, Seg3D software (CIBC, Salt Lake City, Utah), which is an open-source software, to reconstruct polygonal bone models of the tibia, talus, and calcaneus. The reconstructed polygonal bone models from CT images were used for 3D-to-2D registration. A walkway, 0.6 m wide and 4 m long, was constructed using large blocks of high-strength polystyrene foam, of which the density and compressive strength were 30 kg/m^3 and 16 N/cm^2, respectively. Subjects were asked to walk on the walkway barefoot at their self-selected walking speed, as shown in Figure 1. A biplanar fluoroscopic system (KMC-1400ST; Gemss Medical, Kyungki-do, South Korea) was used to obtain fluoroscopic images of the ankle joint complex of the right leg. It was operated at 70 kVp and 20 mA at a rate of 100 frames per second for two seconds with an exposure time of 0.1 milliseconds, which resulted in an effective dose of approximately 0.1 mSv. The angle between the two optical axes of the X-ray tubes was 54°. Recorded images had a 14-bit image depth and resolution of 1024 × 1024 pixels.

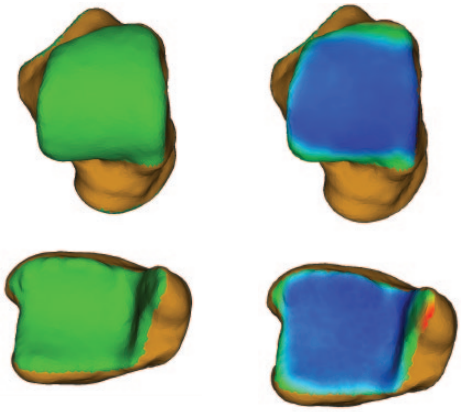

Fig. 2a

Fig. 2b

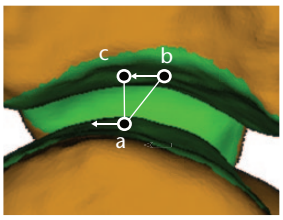

Fig. 2c

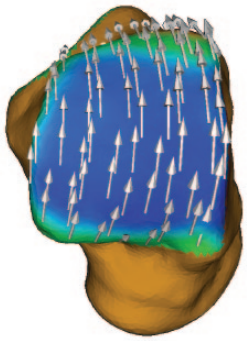

Fig. 2d

a) Subchondral bone surfaces of the talus and tibia in the tibiotalar joint were identified. b) Distance maps were calculated and colour-coded on the surfaces. c) A surface relative velocity vector (SRVV) was calculated for each point in the surface using the vectors to the closest points in two consecutive frames ($\overrightarrow{ac} - \overrightarrow{ab}$), where b and c represent the closest points in the previous and current frames, respectively. d) SRVVs were calculated for sample points in the region of interest.

The polygonal bone models and biplanar images with camera parameters were imported into a virtual 3D environment developed with Matlab (MathWorks, Natick, Massachusetts) and Visualization Toolkit (VTK, Kitware, Clifton Park, New York).[10] The pose of each bone was manually rotated and translated in the 3D environment to match a semi-opaque bone projection image with the bone in the fluoroscopic images in two planes. The number of frames for the stance phase differed between subjects, and the frames of the stance phase were identified manually from fluoroscopic images. Thus, the transformation matrices of the bones were interpolated and resampled at a time interval representing 1% of the total stance time for each subject. The accuracy of the interpolated/resampled translation and rotation were around 0.1 mm and 0.01°, respectively. In quantifying the relative movement, we used transformation matrices at 10% intervals only. Some portions of the foot went outside of the field of view at the terminal stance, in which case the relative movement was calculated from 0% (heel-strike) to 90%.

Relative velocity vectors between two articular surfaces. The contact surfaces of subchondral bone between the tibia and talus on the talar dome, and between the talus and calcaneus on the posterior facet of calcaneus, were extracted from the CT-based polygonal bone models using our in-house anatomical region identification algorithm (Fig. 2a).[20] For each point in a given region of interest, the closest point on the opposite contact surface was identified. For each point (point a) in a region of interest, the closest points in two consecutive frames (points b and c) were identified. A vector joining the two points (points b and c) on the opposite surface was then projected onto the tangential surface at the point (point a) in the region of interest that represented the SRVV of that point (Fig. 2c). Finally, SRVVs were calculated for the sampled points using the fast marching method[21] in the region of interest (Fig. 2d).

Quantification of surface relative velocity vectors. The distribution of SRVVs on contact surfaces, or regions of interest, was quantified for every 10% of the stance phase during walking using the mean relative speed (RS) and the synchronization index (SI_{ENT}) of Shannon entropy (SE).[22,23] Mean relative speed was defined as

$$\text{mean RS} = \frac{1}{n \cdot \Delta t} \cdot \sum_{i=1}^{n} |SRVV_i|$$

where n is the number of SRVVs in a region of interest. The mean duration for the stance phase was 683 milliseconds (SD 52), and thus the Δt was 68.3 milliseconds.

Surface relative velocity vectors were placed into bins ranging from -180° to 180° with a 5° incremental step according to direction. The SE and SI_{ENT} were calculated from the probability of the i-th bin, $p(i)$, as

$$\text{SE} = -\sum_{i=1}^{M} p(i) \ln p(i)$$

$$SI_{ENT} = 1 - \frac{SE}{\ln N}$$

where M is the number of bins with non-zero probability and N is the total number of bins.[24,25] The synchronization index is dimensionless, ranges from 0 to 1, and represents the distribution of angular directions of the SRVV. It is close to 1 if there exists only translational movement between two contact surfaces and the direction of the SRVVs is approximately the same. Conversely, SI_{ENT} is close to 0 if there is rotational movement and the rotation centre is in the central part of the region of interest. Figure 3 shows three representative cases of movement and the corresponding SI_{ENT} values. Surface relative velocity

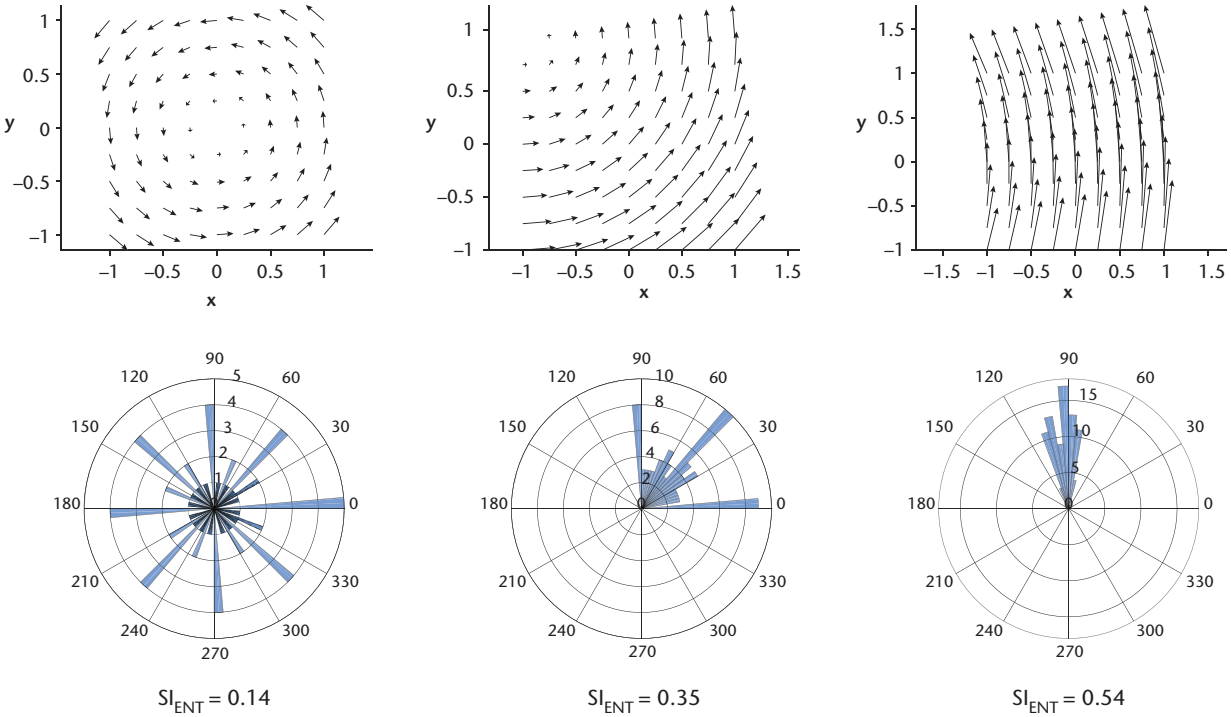

Fig. 3a Fig. 3b Fig. 3c

Three representative cases of surface relative velocity vector (SRVV) distribution in a rectangular region. SRVVs were placed into polar histogram bins to calculate synchronization index (SI_{ENT}). SI_{ENT} was calculated when the rotation centre of the SRVVs was at the a) centre, b) corner, or c) away from the region.

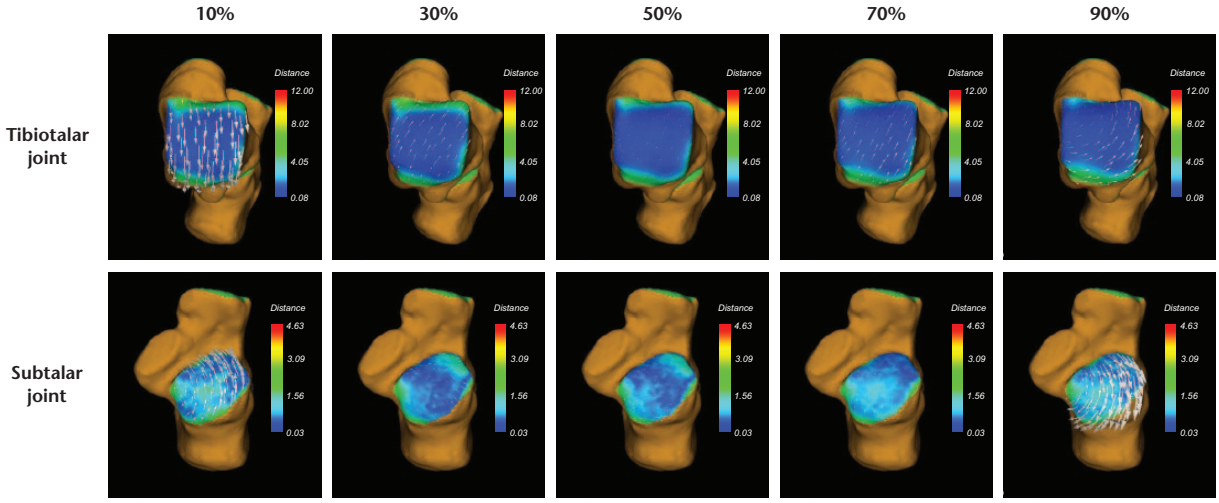

Fig. 4

Surface relative velocity vectors (SRVVs) in the talar dome (top row) and posterior facet of the calcaneus (bottom row) were calculated at 10% intervals to quantify the relative contact movements in the tibiotalar and subtalar joints during walking. Here, we presented the results only for the 10%, 30%, 50%, 70%, and 90% timepoints. The colours on the map represent distances on the contact surface.

vectors were calculated for 81 sample points in the region of interest of a given contact surface. In our study, SI_{ENT} was as low as 0.14 when there was rotational movement around a centre point of the region of interest. Conversely, SI_{ENT} increased to 0.35 and 0.54 when the rotation centres were either at a corner or located away from the region of interest by three times the width, respectively.

Statistical analysis. Descriptive statistical analysis was performed, and data were represented as the means and standard deviations. All datasets were tested for normal distribution using the Kolmogorov–Smirnov test. The mean kinematics data of SI_{ENT} and mean RS at the 10% intervals of the stance phase were compared using repeated-measures analysis of variance (ANOVA) or the Friedman test, according to data normality, and Tukey's test or Wilcoxon's signed-rank test was performed for *post hoc* analysis as appropriate. Bonferroni correction was applied to both *post hoc* tests when determining

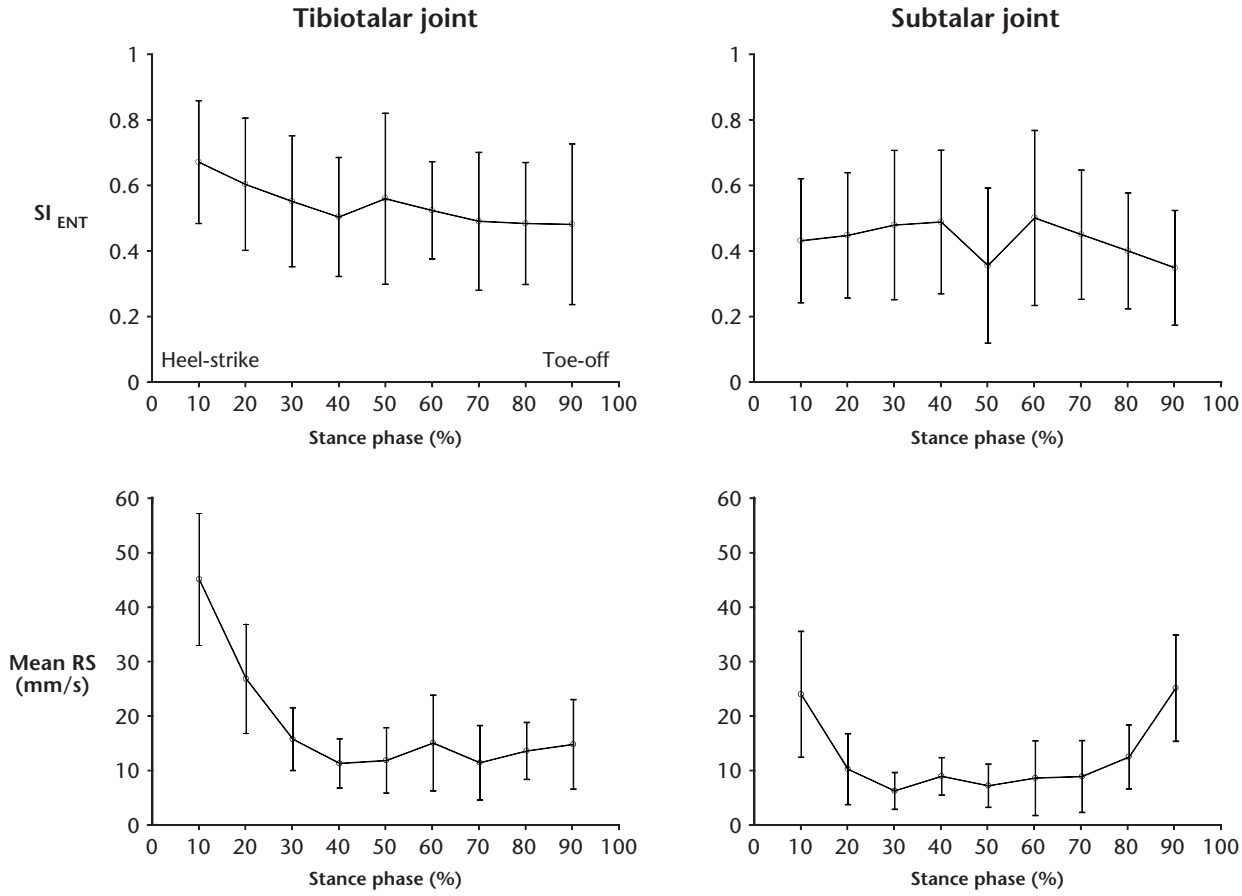

Fig. 5

Graphs showing the means and standard deviations of the synchronization index (SI_{ENT}) and length (mean relative speed (RS)) of surface relative velocity vectors (SRVVs) on articular surfaces were calculated for the tibiotalar and subtalar joints during the stance phase of normal walking.

statistical significance. All statistical analyses were performed using SPSS (version 23, IBM Corp., Armonk, New York), and the level of statistical significance was set at $p < 0.05$ except when Bonferroni correction was applied.

Results

The mean walking speed of the 18 subjects was 1.05 m/s (SD 0.08) at the target position. Figure 4 shows the relative surface movement of the tibiotalar and subtalar joints represented as SRVVs for a representative subject.

The mean RS was significantly higher ($p < 0.01$, Wilcoxon's signed-rank test) during the 0% to 20% period after heel strike than the mean RS corresponding to other periods in the tibiotalar joint (Fig. 5). The synchronization index was 0.64 (SD 0.19) during the 0% to 20% period after heel strike and 0.54 (SD 0.21) for the full stance phase in the tibiotalar joint. The corresponding mean RS values were 45.1 mm/s (SD 11.7) and 26.8 mm/s (SD 9.8) during the 0% to 10% and 10% to 20% periods, respectively, which were significantly larger than those of the remainder of the stance phase ($p < 0.001$, Wilcoxon's signed-rank test). Together, the mean RS and SI_{ENT} data showed that there was a significantly larger degree of translational movement in the early stance of normal walking. For the remainder of the stance period (20% to 90%), the tibiotalar joint exhibited relatively slow translational movement, with a mean RS of 13.4 mm/s (SD 6.7).

The SI_{ENT} of the subtalar joint was 0.43 (SD 0.21) during the full stance phase, but was as low as 0.35 (SD 0.17) during the 80% to 90% stance phase. The mean RS values were 23.9 mm/s (SD 11.3) and 25.1 mm/s (SD 9.5) during 0% to 10% and 80% to 90% of stance phase, respectively, which were significantly higher ($p < 0.001$, Wilcoxon's signed-rank test) compared with the other periods. Thus, the subtalar joint exhibited a significantly larger degree of rotational movement during the early and late stances than those of the remainder of the stance period (10% to 80%), whose mean RS is 8.8 mm/s (SD 5.6).

Discussion

The suggested method of using SRVVs could visualize the relative movements in joints more intuitively and could be used to quantify surface interactions during movement, thus revealing new insights that are not observable in kinematics quantified using the joint coordinate system.[10] To obtain these data, we took advantage of the

high accuracy and non-invasive nature of the recently developed biplanar fluoroscopic measurement method and the 3D-to-2D registration of CT-based polygonal bone models. This approach allowed us to quantify major trends of surface movement, such as rotation and translation, as well as speed. Previous studies on the tibiotalar and subtalar joints frequently utilized a helical axis to describe the kinematics of the ankle joint complex.[13] However, the helical axis only displays the rotational pattern and requires a certain amount of rotational movement to identify the rotational axis in a robust manner.[26] An alternative to the helical axis system is the joint coordinate system that, while able to quantify the rotational and translational movement,[10] is not sufficiently informative with regard to understanding the interactions between bones. On the other hand, the method utilized in this study was able to quantify not only rotational movement, but also translational movement on the contact surface, which allowed for better understanding of the mechanical interactions between surfaces. Importantly, this approach has many potential implications for the study of degenerative diseases involving the articular surface, such as osteoarthritis.[1]

While the SRVVs allow for intuitive visualization of the movement vector field on a contact surface, the SI_{ENT} of the Shannon entropy was originally suggested to measure synchronization of the relative phase distribution of magnetoencephalograms[25] and musical beats.[24] However, SI_{ENT} is also appropriate for understanding the level of synchronization among movement vectors on a contact surface, with a SI_{ENT} of 0 representing pure rotation around the centre of a region of interest and a SI_{ENT} of 1 representing pure translation. Computation of the Shannon entropy depends on the number of histogram bins and sampling points on contact surfaces. In calculating the Shannon entropy, artefacts can be removed by fixing the number of histogram bins and increasing the number of sampling points to converge the probability of each bin.[23] In our study, a mean of 80.7 points and 82.8 points were sampled in the talar dome and posterior facet of calcaneus, respectively, which were placed into 72 bins to calculate the SI_{ENT} in each region of interest.

According to the results of our study, translational movement was dominant on the contact surface in the tibiotalar joint, with a mean SI_{ENT} of 0.54 (SD 0.21). Translational movement was relatively high during the first 20% of the stance phase in the tibiotalar joint, with a mean RS of 36.0 mm/s (SD 14.2). This finding was attributed to the fast plantar flexion that takes place during the heel strike, which is during the first 10% of the stance, followed by the relatively fast dorsiflexion of the subsequent 10% of the stance.[11]

There have been frequent reports of rotation of the tibiotalar joint in the sagittal plane, which may represent translational movement from the perspective of the surface. According to our results, the relative movement in the tibiotalar surfaces is mostly translational movement due to plantar/dorsi flexion in the joint, but it also included small rotational movements with a mean SI_{ENT} of 0.54 (SD 0.21) due to internal/external rotation, which should be a consequence of the conical shape of the talar dome.[27] Low SI_{ENT} values indicate internal/external rotation and high SI_{ENT} values indicate plantar/dorsi flexion in the tibiotalar joint. Interestingly, mean RS reached a minimum of around 40% of the stance phase, which was maintained until the toe-off, which may suggest that the tibiotalar joint becomes rigid and acts as a lever arm during the push-forward period. On the other hand, we found that rotational movement was dominant on the surface of the subtalar joint, with a SI_{ENT} between 0.35 and 0.5. Qualitatively, the rotation centre was at the medial anterior border of the posterior facet of calcaneus, which conformed to the location of the helical axis of subtalar joints found in cadaveric studies.[14] In addition, according to the mean SI_{ENT} and mean RS data, the rotational movement of both the early and late stance of the subtalar joint during walking were significantly faster than that of the mid-stance.

The kinematic observations of the tibiotalar and subtalar joints in the present study should provide a better understanding of the symptoms described by patients with arthritis in these joints. For example, if the range of movement of the tibiotalar joint is limited in patients with ankle arthritis, they should feel uncomfortable only during the initial stance phase. On the other hand, if the range of movement of the subtalar joint is limited due to subtalar arthritis, patients should describe symptoms during both the early and late stance phase. Certainly, the symptoms can also be affected by joint kinetics such as joint reaction forces.[5] According to our results, rotational movement was considerably higher at the terminal stance in the subtalar joints. At this point, the contact force at the ankle joint complex is as high as six times the body weight at the terminal stance of walking,[2] which is the only timepoint when the movement of the subtalar joint is greater than that of the tibiotalar joint (mean RS 25.1 mm/s *vs* 14.8 mm/s).

There were several limitations in this study. We tested subjects from a relatively homogeneous group in terms of gender, age, height, and weight. In addition, fluoroscopic image acquisition was performed in a radiation-shielded space that limited the length of our walking track to four metres. This track length also affected the mean walking speed of the subjects at the target position. The duration of the stance phase varied between subjects, but the mean duration was used to calculate the SRVV for all subjects, which could affect the accuracy of the SRVVs of individual subjects. Nevertheless, its effects on our results should be minimal because our comparisons were made between normalized timepoints and not

between subjects. Another limitation of this study was that the 3D-to-2D matching was performed manually, which may have introduced errors of bias and precision. However, registration of the tibia, talus, and calcaneus for full stance phase by three independent observers led to an intraclass correlation coefficient (ICC) between observers of 0.94 (SD 0.05) and 0.99 (SD 0.01), for translation and rotation, respectively.

In this study, we presented an approach for quantifying the kinematics of the ankle joint complex at the level of the subchondral bone surface based on SRVVs on a contact surface, which is a potential method for better understanding the interaction in the ankle joint complex during daily activity. Our description of surface interactions should provide greater insight into degenerative joint diseases such as osteoarthritis at the level of the articular surface.

References

1. **Andriacchi TP, Mündermann A, Smith RL, et al.** A framework for the in vivo pathomechanics of osteoarthritis at the knee. *Ann Biomed Eng* 2004;32:447-457.
2. **Prinold JA, Mazzà C, Di Marco R, et al.** A patient-specific foot model for the estimate of ankle joint forces in patients with juvenile idiopathic arthritis. *Ann Biomed Eng* 2016;44:247-257.
3. **Sarrafian SK.** Biomechanics of the subtalar joint complex. *Clin Orthop Relat Res* 1993;290:17-26.
4. **Maceira E, Monteagudo M.** Subtalar anatomy and mechanics. *Foot Ankle Clin* 2015;20:195-221.
5. **Delahunt E, Monaghan K, Caulfield B.** Changes in lower limb kinematics, kinetics, and muscle activity in subjects with functional instability of the ankle joint during a single leg drop jump. *J Orthop Res* 2006;24:1991-2000.
6. **Hertel J.** Functional anatomy, pathomechanics, and pathophysiology of lateral ankle instability. *J Athl Train* 2002;37:364-375.
7. **Lundberg A.** Kinematics of the ankle and foot. In vivo roentgen stereophotogrammetry. *Acta Orthop Scand Suppl* 1989;233:1-24.
8. **de Asla RJ, Wan L, Rubash HE, Li G.** Six DOF in vivo kinematics of the ankle joint complex: application of a combined dual-orthogonal fluoroscopic and magnetic resonance imaging technique. *J Orthop Res* 2006;24:1019-1027.
9. **Wang B, Roach KE, Kapron AL, et al.** Accuracy and feasibility of high-speed dual fluoroscopy and model-based tracking to measure in vivo ankle arthrokinematics. *Gait Posture* 2015;41:888-893.
10. **Koo S, Lee KM, Cha YJ.** Plantar-flexion of the ankle joint complex in terminal stance is initiated by subtalar plantar-flexion: A bi-planar fluoroscopy study. *Gait Posture* 2015; 42:424-429.
11. **Arndt A, Westblad P, Winson I, Hashimoto T, Lundberg A.** Ankle and subtalar kinematics measured with intracortical pins during the stance phase of walking. *Foot Ankle Int* 2004;25:357-364.
12. **Lundgren P, Nester C, Liu A, et al.** Invasive in vivo measurement of rear-, mid-and forefoot movement during walking. *Gait Posture* 2008;28:93-100.
13. **Sheehan FT.** The instantaneous helical axis of the subtalar and talocrural joints: a non-invasive in vivo dynamic study. *J Foot Ankle Res* 2010;3:13.
14. **Beimers L, Tuijthof GJ, Blankevoort L, et al.** In-vivo range of motion of the subtalar joint using computed tomography. *J Biomech* 2008;41:1390-1397.
15. **Andriacchi TP, Koo S, Scanlan SF.** Gait mechanics influence healthy cartilage morphology and osteoarthritis of the knee. *J Bone Joint Surg [Am]* 2009;91-A(Suppl 1):95-101.
16. **Koo S, Rylander JH, Andriacchi TP.** Knee joint kinematics during walking influences the spatial cartilage thickness distribution in the knee. *J Biomech* 2011;44:1405-1409.
17. **Li G, Wuerz TH, DeFrate LE.** Feasibility of using orthogonal fluoroscopic images to measure in vivo joint kinematics. *J Biomech Eng* 2004;126:313-318.
18. **Akbarshahi M, Schache AG, Fernandez JW, et al.** Non-invasive assessment of soft-tissue artifact and its effect on knee joint kinematics during functional activity. *J Biomech* 2010;43:1292-1301.
19. **Anderst WJ, Tashman S.** Using relative velocity vectors to reveal axial rotation about the medial and lateral compartment of the knee. *J Biomech* 2010;43:994-997.
20. **Phan CB, Koo S.** Predicting anatomical landmarks and bone morphology of the femur using local region matching. *Int J Comput Assist Radiol Surg* 2015; 10:1711-1719.
21. **Peyre G, Cohen LD.** Geodesic remeshing using front propagation. *Int J Comput Vis* 2006;69:145-156.
22. **Shannon CE.** The mathematical theory of communication. *ATT Tech J* 1948;27:379–423.
23. **Xu L, Lee TY, Shen HW.** An information-theoretic framework for flow visualization. *IEEE Trans Vis Comput Graph* 2010;16:1216-1224.
24. **Fujii S, Schlaug G.** The Harvard Beat Assessment Test (H-BAT): a battery for assessing beat perception and production and their dissociation. *Front Hum Neurosci* 2013;7:771.
25. **Tass P, Rosenblum MG, Weule J, et al.** Detection of n: m phase locking from noisy data: Application to magnetoencephalography. *Phys Rev Lett* 1998;81:3291-3294.
26. **Graf ES, Wright IC, Stefanyshyn DJ.** Effect of relative marker movement on the calculation of the foot torsion axis using a combined Cardan angle and helical axis approach. *Comput Math Methods Med* 2012;2012:368050.
27. **Norkus SA, Floyd RT.** The anatomy and mechanisms of syndesmotic ankle sprains. *J Athl Train* 2001;36:68-73.

Funding Statement

- This work was financially supported by Projects for Research and Development of Police Science and Technology through CRDPST and KNPA (PA-C000001) and by the Basic Science Research Program through the NRF (2017R1A2B2010763) funded by the Ministry of Science and ICT of South Korea. This research was also supported by the International Joint Technology Development Program through the KIAT (No. N0001721) funded by the Ministry of Trade, Industry, and Energy of South Korea.

Author Contribution

- C-B. Phan: Designing the study, Interpreting the data, Writing the manuscript.
- D-P. Nguyen: Designing the study, Interpreting the data, Writing the manuscript.
- K. M. Lee: Designing the study, Interpreting the data, Writing the manuscript.
- S. Koo: Designing the study, Interpreting the data, Writing the manuscript.

Conflict of Interest Statement

- None declared